Nuclear Instruments and Methods in Physics Research A 619 (2010) 150–153

Contents lists available at ScienceDirect

Nuclear Instruments and Methods in Physics Research A

journal homepage: www.elsevier.com/locate/nima

The effects of cosmic ray filtering on low intensity X-ray CCD data

L.F. Smale [a,*], C.T. Chantler [a], L.T. Hudson [b]

[a] School of Physics, University of Melbourne, Victoria, 3010, Australia
[b] National Institute of Standards and Technology, Gaithersburg, MD 20899-8422, USA

ARTICLE INFO

Available online 14 January 2010

Keywords:
X-ray detectors
Cosmic rays

ABSTRACT

Various methods exist to filter cosmic rays from X-ray CCD images with weak X-ray spectra. Distortions of the characteristics of a spectral profile such as peak centroid and relative integrated peak intensities must be kept to a minimum. Optimum methods are those minimising error bars and widths on the final centroid determination and on relative intensities which remain consistent with the widths for unfiltered data. A cluster method, a linear correlation method and a combination of both were examined using H-like Ti collected at the NIST EBIT. The cluster method is a strong filter but appears to distort centroids and relative intensities. The linear correlation method filters less and distorts less. The strongest filtering is to use both yielding the highest signal-to-noise while enhancing apparent distortions. All methods appear fairly robust. Strong cosmic-ray filters with minimal distortion of X-ray spectra can increase the precision of X-ray CCD measurements and enhance the resulting physical insight.

1. Introduction

X-ray CCD images of weak X-ray spectra can be analysed to remove significant noise signals such as from cosmic rays [1–3]. Distortions of the characteristics of a spectral profile such as peak centroid and relative integrated peak intensities must be kept to a minimum with these methods, or potential accuracy and physical insight will be lost. An ideal method will minimise broadening and uncertainty of final centroid determination and of relative intensities consistent with the distribution for the unfiltered data. A cluster method, a linear correlation method and a combination of both were examined using H-like Ti X-rays collected at the NIST EBIT.

X-ray CCD sensors are important in a wide range of experiments from X-ray astronomy to atomic physics. Extracting significant information from X-ray CCD images is therefore quite a general and important problem. Cosmic ray tracks are a significant source of noise in X-ray CCD images with significant integration times. Automated techniques to differentiate these background tracks from X-ray signals of direct interest in a particular investigation need further development.

Reducing the noise from cosmic rays has been an important step in the analysis of polarisation data for measuring the Lamb shift of He-like Ti [4]. Lamb shift and general high-accuracy experiments require detailed characterisation of systematics and detector performance [5,6]. In the experimental setup [7], there were two Johann geometry spectrometers [8,9] attached to perpendicular ports of the NIST EBIT (Fig. 1). The main spectrometer had a vertical configuration with a backgammon type multi-wire proportional counter as the detector and the secondary had a horizontal configuration with an X-ray CCD detector. Spectra observed include He-like Ti and a very low intensity H-like Ti source. Therefore, in the CCD detector, cosmic rays were a significant source of noise. The CCD used had background levels, defined as a fixed-pattern noise on top of a thermal pedestal, partially due to typical radiation damage accumulated in the detector over time. To correct for these effects, we need to characterise the background and remove it. A typical raw data CCD image is shown in Fig. 2. Note that many such images must be processed and the results added to create a spectrum with significant statistics.

2. Mean background determination

Each data image from the CCD needs to be separated into three computational masks, representing the regions and nature of constituent pixel signals. We are searching for a mask (a pixel intensity pattern) which represents the background or electronic noise or damage signal of the CCD detector, a mask which represents the cosmic ray events for exclusion from the signal, and a mask of the 'true' X-ray signals of interest. Ten exposures of the background were taken during the experiment. All the background images were normalised to the brightest background image through linear intensity histogram matching.

* Corresponding author.
E-mail address: lucasfs@physics.unimelb.edu.au (L.F. Smale).

0168-9002/$ - see front matter © 2010 Published by Elsevier B.V.
doi:10.1016/j.nima.2010.01.007

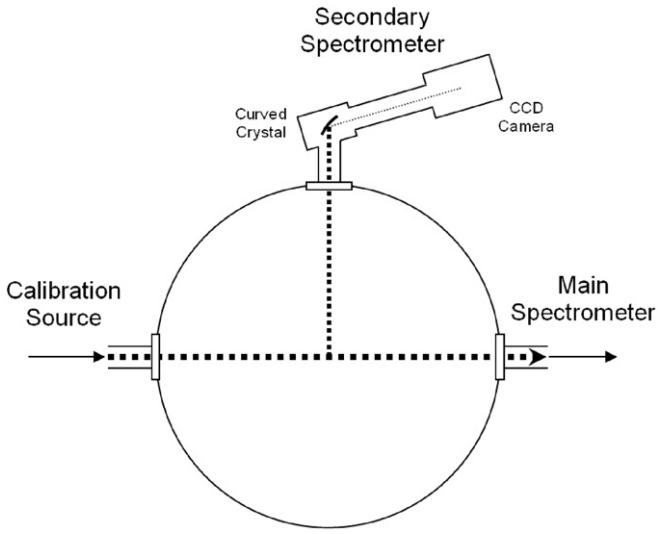

Fig. 1. The experimental setup showing the horizontal configuration of the secondary spectrometer with X-ray CCD detector attached.

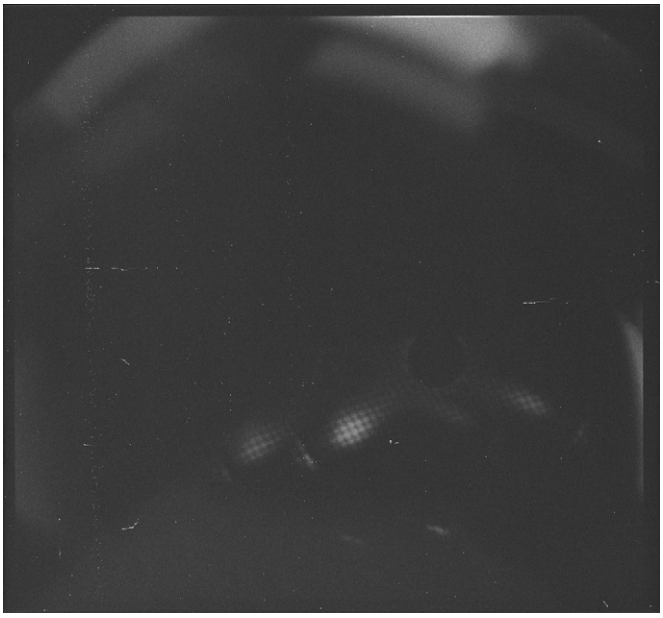

Fig. 2. Raw image data of He-like Ti, showing the background pattern as well as cosmic rays and the X-ray signal.

The intensity histograms of every CCD image examined in the experiment had two disjoint (bimodal) peaks. Therefore, to scale each background image to the brightest background image, the means of each of these two peaks for both images were found. The intensity of each background was linearly transformed such that the means of the two peaks of each background matched those of the brightest background. This will correct for variations in dead-time, temperature drifts or integration times and will hopefully avoid secondary distortion.

Therefore, for each pixel location there is a set of samples of intensities (grey level) taken from normalised background images. An accurate measure of the background was taken to be the mean of this set, excluding elements that represent cosmic-ray intensities. These cosmic ray events are outliers in the sample distribution. Therefore, for each pixel, outliers were removed. The mean and standard deviation of the remaining grey level distribution then defined the background distribution, and the scale was normalised to the background level mean and standard deviation of the distribution.

To detect outlier sample intensities within the set of normalised background image intensities, the set was divided into two new subsets: the set of intensities above the midpoint between the mean and maximum of the set and the set of intensities below that midpoint. If a *t*-test for the consistency of these subsets shows they are *inconsistent*, we take the second set to represent the background, otherwise we take the original set to be a sample of the background distribution.

3. Background subtraction

Typically, there will be a background average image, and a series of data-containing images. However, these backgrounds do not have the same brightness (grey-scale) because of drift in laboratory temperature for example. To subtract the mean background from a raw CCD image, the mean background was normalised to the image through a scaling of intensity.

For each image, a difference image was created by subtracting the normalised background image from the image. The grey level distribution of the difference image is peaked around 0 but is not precisely 0 because of noise in the component images. The pixels corresponding to this peak around 0 show an absence of cosmic rays and X-rays. That is, they appear to be due to thermal noise or background patterning. A cutoff value greater than the noise but less than the signal was therefore chosen to define a background distribution mask. All pixels that had an intensity above the cutoff were kept in a 'Possible X-ray Signal Mask' PXSM (Fig. 3 shows the sum of the PXSMs of all He-like Ti data images). The intensity of each pixel marked by the PXSM in the difference image is assumed to be proportional to the energy deposited (by X-rays or cosmic rays) in that CCD pixel in the collection time of the image.

4. Cosmic ray filters

Three filters where examined: a cluster method, a linear correlation method using Hough transforms and a combination of

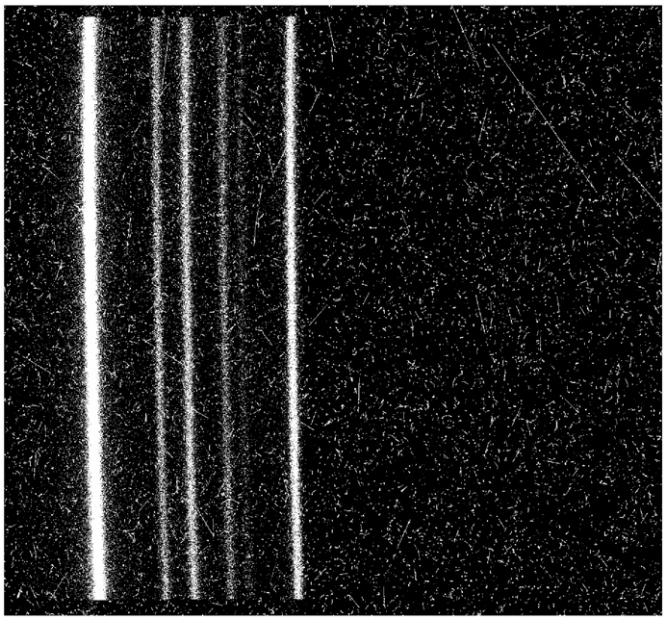

Fig. 3. The sum of the Possible X-ray Signal Masks (PXSMs) for the He-like Ti data. This represents the unfiltered data.

both. In the cluster method, continuous clusters of pixel signals in the PXSM whose combined energy deposition is greater than a chosen cutoff are marked as cosmic ray events and filtered out. The cutoff is chosen through an examination of X-ray events identified by eye in a few images. The linear correlation method identifies linear tracks in the PXSM that need not be continuous clusters. It uses Hough transforms and Hough back-projection.

4.1. Hough transform

The Hough transform [10] is a robust line recognition technique. The set of all straight lines possible in the image is parameterised by a set of two numbers. Each axis of a Hough space image represents a parametrisation of the line. Therefore each 2D point in the Hough space represents a particular (distinct) line in the image. The value of the Hough transformed image at a particular point (parameter set) is the number of non-zero pixels in the source image that are elements of the line represented by that parameter set. An approximately straight line can then be recognised by a peak in the Hough image.

The value of the Hough back-projected image at a particular pixel is calculated from the group of points in the Hough transform whose corresponding lines go through that particular pixel. The value of the image is the sum of intensities of this group.

4.2. Linear correlation method

There are linear correlations of pixels in the PXSM other than cosmic rays—most importantly the spectral lines of the positional-dependent X-rays of the signal. These points can be recognised and removed from misidentification as cosmic rays because they are normally isolated from each other (i.e. they are not usually overlapping clusters) due to the low intensity of the spectral lines. Isolated points in the PXSM are points with less than 3 on-pixels in the surrounding 5×5 sub-mask. The remaining loosely clustered points are included in the 'Possible Cosmic Ray Mask' PCRM.

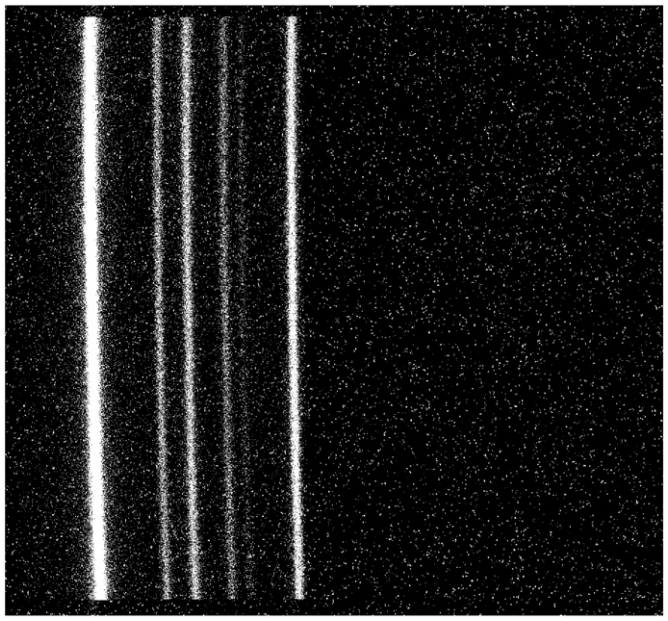

Fig. 4. The sum of the results of applying the linear correlation filter method to each He-like Ti data image.

We Hough transform the resulting PCRM, zero the pixels of the Hough image which are less than a cutoff (chosen to be five). This means that there must be five pixels in a discontinuous line on the PCRM for such a collection of points to be recognised as a line. We then Hough back-project this cut Hough transform image into the original image space. Areas of high intensity represent pixels in approximately collinear (confined) patterns in the original PCRM.

All pixels with a Hough back-projection intensity below a cutoff (chosen to be 150 but robust within a wide range, a good balance between identifying confined linear correlations and correlations between very isolated clusters) that are marked by the PCRM are marked as linearly correlated cosmic rays and filtered out as cosmic ray events. Fig. 4 shows the sum of the results of the linear correlation method applied to each He-like Ti data image.

The spectral lines were not perfectly vertical on the CCD image due to the difficulty of rotating the CCD camera once the spectrometer is evacuated. To sum the spectra and see the signal after a column sum, the image was rotated in order to minimise the width of the strongest peak in the spectrum. Robustness of

Table 1
The signal-to-noise ratio of each peak increases with filtering from A (raw data with background normalisation and rotation) to B (Hough transform with background normalisation and rotation) to C (cluster method with background normalisation and rotation) to D (B and C combined).

Peak #	Peak signal to noise			
	Set A	Set B	Set C	Set D
1	1.287	3.330	10.083	10.651
2	2.357	4.891	16.965	17.686
3	8.154	16.922	57.946	60.391
4	1.451	3.374	12.360	13.025
5	3.813	7.779	26.118	27.367
6	2.464	4.144	13.250	13.996
7	2.191	4.884	16.767	17.584
8	1.693	3.357	10.526	11.040

The noise level is given by the fitted constant background coefficient.

Table 2
The full width half maximum and the dependence on filtering method.

Peak #	FWHM (column channels)			
	Set A	Set B	Set C	Set D
1	8(1)	5.6(2)	6.4(2)	6.4(2)
2	6.1(6)	5.6(1)	5.9(3)	5.8(2)
3	6.3(6)	5.83(5)	6.0(3)	5.96(5)
4	6.0(7)	6.3(2)	7.0(2)	7.0(2)
5	5.7(7)	6.00(7)	6.0(3)	5.8(2)
6	8.6(8)	7.4(4)	7.9(1)	7.7(2)
7	6.6(7)	6.3(3)	6.2(3)	6.2(1)
8	5.2(6)	5.8(1)	6.7(3)	6.8(1)

The FWHM is most stable with linear correlation filtering (set B).

Table 3
The centroid of the strongest peak, relative to Set A position, appears to remain stable within about one σ.

3rd peak centroid (column channels)			
Set A	Set B	Set C	Set D
0.00(8)	0.10(7)	0.10(7)	0.10(7)

Table 4
This table shows the peak position and intensity of each peak across all filtering methods relative to the strongest peak (the third peak).

Peak #	Relative peak position (column channels)				Relative intensity			
	Set A	Set B	Set C	Set D	Set A	Set B	Set C	Set D
1	−151.7(5)	−152.6(3)	−153.0(2)	−152.9(2)	0.20(2)	0.20(2)	0.19(1)	0.19(1)
2	−23.1(2)	−23.2(2)	−23.1(2)	−23.0(2)	0.28(2)	0.28(2)	0.29(1)	0.29(2)
4	30.2(3)	30.1(2)	30.5(2)	30.4(2)	0.17(2)	0.21(2)	0.25(1)	0.25(1)
5	68.8(1)	69.2(2)	69.4(1)	69.4(1)	0.41(2)	0.47(2)	0.46(2)	0.46(2)
6	121.9(3)	121.6(2)	121.8(2)	121.8(2)	0.41(3)	0.30(2)	0.30(2)	0.30(2)
7	197.4(2)	197.1(2)	197.1(2)	197.1(2)	0.28(2)	0.31(2)	0.30(2)	0.31(1)
8	306.1(2)	306.0(2)	306.0(2)	306.0(2)	0.17(1)	0.20(1)	0.20(1)	0.21(1)

The dimensionless relative intensity is the integrated area of a peak relative to that of the strongest peak. The relative peak position measures the consistency within errors of the relative centroid locations and hence of the calibration. The second strongest (peak 5) shifts by circa 2-3σ in position, doubling with Cluster Filtering. Peaks 4, 5 and 6 in particular show strong dependencies with filtering.

this simple rotation optimisation was tested by shifts in angular rotation from the final result by 0.25°.

5. Results

Four sets of results from the Rydberg series of H-like Ti data were generated for comparison: no cosmic-ray filtering (set A); Linear Correlation filtering (set B); Cluster filtering (set C); combined Linear Correlation and Cluster filtering (set D). Each set of results was created through event identification, spectrum creation (through a rotation and column sum of all the event images), and spectrum fitting (the fit function was a sum of 8 Voigt functions with a common gaussian width and a constant background for the noise).

Table 1 shows the signal-to-noise ratio for each peak in each filter method. The noise estimate was given by the constant background level from the fit. This measures the strength of the filter. The combination filter was stronger than either sub-filter. Hence the sub-filters filter out different components of the cosmic ray noise and of the X-ray signal (as was expected). Table 1 demonstrates that all methods yielded dramatic improvement in separating real (X-ray) signal from noise or correlated components, by factors up to 7–9.

Table 2 illustrates the dependence of the peak full width half maximum on filtering method. The fitted centroid and width of the strongest peak (peak 3) is stable under all methods of filtering (Table 3), supporting the idea that for strong lines each of these approaches has a valid construction. The raw rotated image (set A) may be broadened by artificial (poor) definitions of the background and hence FWHM, by the noise or cosmic rays themselves, and by poor definitions of the lines due to statistics, which might yield a larger width. However, filtered data should be stable in FWHM if all processing has avoided distortion, and conversely should always be larger if the processing has involved distortion and loss of definition of peaks. Results suggest that the weakest components (1, 4 and 8) increase their apparent FWHM from set B to C to D. This suggests that weak peaks are distorted and that Set B minimises this effect.

Table 4 gives the relative peak position and relative intensity as measures of peak distortion. Relative integrated intensities are normalised to the strongest peak in this table. The distortions of intensity generally increase with the strength of the filter, in support of the observations relating to the FWHM. The second strongest peak (5) shifts by circa 2-3σ (B) in relative intensity, with the shift doubling with the energy cluster filtering (C). Peaks 4, 5 and 6 in particular show strong dependencies with filtering, both with integrated relative intensities and with centroid location. Of course, both of these measures are the primary outputs for calibration of scientific results using a CCD detector.

6. Conclusion

The stability and robustness of filtering cosmic-ray noise from low intensity X-ray data from CCD cameras is an important problem. Three filtering methods have been compared. The FWHM of the spectral line is most stable (most narrow) with the Hough transform (B). Cluster methods (C) may increase noise and widths on weak lines. The cluster method is a strong filter compared to the linear correlation filter but can distort centroids and relative intensities. The linear correlation method appears to distort less. The strongest filtering is achieved by combining both filters in which case the distortions are typically enhanced further. All methods appear moderately robust under test conditions on real data. The tentative conclusion is that the minimum filter (B) is the preferred for weak signals, as it appears to avoid distortions. However, more work is clearly needed both to optimise and investigate these and further alternate models in the presence of important but weak signals, for CCD investigations or indeed for any pixel-based imaging.

References

[1] L.T. Hudson, J.D. Gillaspy, J.M. Pomeroy, C.I. Szabo, J.N. Tan, B. Radics, E. Takacs, C.T. Chantler, J.A. Kimpton, M.N. Kinnane, L.F. Smale, Nuclear Instruments and Methods in Physics Research A 580 (2007) 33.
[2] D. Groom, Experimental Astronomy 14 (1) (2002) 45.
[3] M. Donahue, C.A. Scharf, J. Mack, Y.P. Lee, M. Postman, P. Rosati, M. Dickinson, G.M. Voit, J.T. Stocke, The Astrophysical Journal 569 (2002) 689.
[4] C.T. Chantler, Radiation Physics and Chemistry 71 (2004) 611.
[5] C.T. Chantler, J.M. Laming, D.D. Dietrich, W.A. Hallett, R. McDonald, J.D. Silver, Physical Review A (Atomic, Molecular, and Optical Physics) 76 (4) (2007) 042116.
[6] C.T. Chantler, J.M. Laming, J.D. Silver, D.D. Dietrich, P.H. Mokler, E.C. Finch, S.D. Rosner, Physical Review A (Atomic, Molecular, and Optical Physics) 80 (2) (2009) 022508.
[7] C.T. Chantler, D. Paterson, L.T. Hudson, F.G. Serpa, J.D. Gillaspy, E. Takács, Physical Review A 62 (4) (2000) 042501.
[8] A. Henins, Review of Scientific Instruments 58 (1987) 1173.
[9] S. Brennan, P.L. Cowan, R.D. Deslattes, A. Henins, D.W. Lindle, B.A. Karlin, Review of Scientific Instruments 60 (1989) 2243.
[10] R.O. Duda, P.E. Hart, Commun. ACM 15 (1) (1972) 11.